Magnetic anisotropy and Mössbauer effect studies of $YFe_{11}Ti$ and $YFe_{11}TiH$

2001 J. Phys.: Condens. Matter 13 8161

(http://iopscience.iop.org/0953-8984/13/35/321)

INSTITUTE OF PHYSICS PUBLISHING JOURNAL OF PHYSICS: CONDENSED MATTER

J. Phys.: Condens. Matter **13** (2001) 8161–8170 PII: S0953-8984(01)22657-5

Magnetic anisotropy and Mössbauer effect studies of $YFe_{11}Ti$ and $YFe_{11}TiH$

I S Tereshina[1,2], P Gaczyński[2], V S Rusakov[1], H Drulis[2,4], S A Nikitin[1,3], W Suski[2,3], N V Tristan[3] and T Palewski[3]

[1] Physics Department of Moscow State University 119899, Moscow, Russia
[2] Polish Academy of Sciences, Trzebiatowski Institute of Low Temperature and Structure Research, PO Box 1410, 50-950 Wroclaw, Poland
[3] International Laboratory for High Magnetic Fields and Low Temperatures, 53-421 Wroclaw, Poland

E-mail: drulis@int.pan.wroc.pl

Received 8 March 2001
Published 16 August 2001
Online at stacks.iop.org/JPhysCM/13/8161

Abstract

The magnetic properties and ^{57}Fe Mössbauer spectra of the compounds $YFe_{11}TiH_x$ ($x = 0$, 1) were investigated. The magnetocrystalline anisotropy of $YFe_{11}Ti$ and its hydride was studied by analysing the hard and easy magnetization curves of single crystal samples in the temperature range 4.2–300 K. The spontaneous magnetization was determined in wide temperature range 4.2–650 K. It is established that at $T = 4.2$ K magnetic anisotropy constants K_1 and K_2 for $YFe_{11}TiH_1$ single crystal reach values of 25.8 K f.u.$^{-1}$ and 0.24 K f.u.$^{-1}$, respectively. The Mössbauer effect spectra of $YFe_{11}Ti$ and its hydride were analysed in terms of a model which takes into account the local environment of Fe atoms on three crystallographic sites (8f, 8j and 8i) and an influence of the random distribution of titanium on the 8i site. Upon hydrogenation both the hyperfine fields and the isomer shifts increase. These results are discussed in terms of the hydrogen-induced unit cell expansion and the electron charge transfer from the conduction band onto the H atoms.

1. Introduction

Investigations have shown that $RFe_{11}Ti$ compounds, which crystallize in the tetragonal $ThMn_{12}$ type structure, can absorb some quantities of hydrogen gas in a gas–solid reaction and form the corresponding metal hydrides [1, 2]. In this structure the following interstitial sites: the octahedral 2b (0;0;1/2) and the tetrahedral 8h (1/4;1/4;0), adjacent to the rare earth atoms in the lattice, are available for atoms like hydrogen, nitrogen or carbon. All these

[4] Author to whom correspondence should be addressed.

so-called interstitial atoms were found to have a remarkable effect on the increase of the Curie temperature, enhancement of the saturation magnetization and modification of magneto-crystalline anisotropy (MCA) in this type of intermetallic compounds [3, 4].

In the $RFe_{11}Ti$ compounds both the rare earth and the 3d-metal sublattices contribute to the total magnetic anisotropy. The anisotropy of the former sublattice is due to the electrostatic interactions of the 4f electrons with the crystal electric field potential created by the electric charges of the surrounding ions. The iron contribution is more complex and is not well understood yet. The detailed understanding of the Fe sublattice anisotropy is a formidable task of the theory both in the host and in the interstitially modified rare-earth–transition-metal compounds. It is assumed to be attributed to band structure effects associated with the incompletely quenched 3d orbital moment and spin–orbit coupling. The yttrium compounds are often studied in order to evaluate the contribution of the transition metal to the global magnetic properties, since the yttrium can be regarded as a non-magnetic rare earth having an atomic radius similar to the elements from the middle of the rare earth series. In $YFe_{11}Ti$ and $YFe_{11}TiH$ only the Fe atoms have a magnetic moment and only the Fe atoms are responsible for the magnetic structure. Insertion of hydrogen in $YFe_{11}Ti$ leads to an increase of the Curie temperature, the saturation magnetization and the value of the ^{57}Fe hyperfine fields [4, 5]. One way to explain these observations can be the volume effect [5]. Due to the volume expansion upon hydrogenation the increase of the Fe–Fe distances and narrowing of Fe-3d band will take place. These changes usually are responsible for the increase of the Curie temperature, T_c, and the increase of the saturation magnetization. However, apart from the unit cell expansion one should also remember that the hydrogen atoms can donate their electrons to the iron sd-bands or can depopulate them as well [6–8]. In this case, appropriate (opposite to each other) changes of the hyperfine fields and isomer shift in the Mössbauer experiments will be detected.

Several investigators [9–11] have studied the magnetocrystalline anisotropy (MCA) in the $YFe_{11}Ti$ compound. The second-order magnetocrystalline anisotropy constant $K_1(T)$ has, for instance, been estimated for magnetically aligned $YFe_{11}Ti$ powder samples [9]. The $K_1(T)$ and $K_2(T)$ anisotropy constants were also estimated for a $YFe_{11}Ti$ single crystal from the magnetization isotherms [10] and from the experimental torque curves [11]. It was established that at $T = 4.2$ K they reach values of 24 ± 0.2 K f.u.$^{-1}$ and 0.44 ± 0.2 K f.u.$^{-1}$, respectively [10].

Here, for the first time, we report the anisotropy properties of $YFe_{11}TiH$ hydride single crystals. Besides, in this paper the Mössbauer spectra of $YFe_{11}Ti$ and $YFe_{11}TiH$ will be given and analysed in terms of the crystallographic structure and sites occupancy.

2. Experimental details

Intermetallic samples prepared as described in reference [12] were used to synthesize the hydride samples in a gas–solid reaction. Hydrogenation was carried out in a stainless steel chamber under a pressure of 0.3 MPa of high-purity hydrogen gas at temperatures up to 300 °C. A short thermal activation was needed to initiate the hydrogen absorption process. The final hydrogen content was determined by a volumetric method. The hydrogen concentration was near to one H atom per formula unit: $YFe_{11}TiH_{1-y}$ ($y \approx 0.05$). The obtained hydride single crystals were of high quality.

The orientation of the $YFe_{11}TiH_{1-y}$ single crystal along the symmetry axes has been performed using the x-ray diffraction method. Magnetization measurements were performed with a SQUID magnetometer in fields up to 5.5 T and in the temperature range 1.5–300 K.

The Curie temperature of the $YFe_{11}TiH_x$ ($x = 0$, 1) compounds were determined from the thermomagnetic analysis at low external fields (0.1 T) in the temperature range 300–700 K.

The ^{57}Fe spectra were taken at temperatures 20 K and 295 K with a conventional constant acceleration spectrometer. The γ radiation source was ^{57}Co in an Rh matrix. The absorber was prepared by grinding the sample to a fine powder with MgO to ensure a constant surface density with an optimal thickness of 9 mg Fe cm^{-2}. The velocity scale was calibrated by means of a metallic α-iron foil at room temperature. The isomer shift values are given relative to α-Fe at $T = 295$ K. The spectra were analysed by the least-squares fits of the experimental results using the pseudo-Voigt approximation of Mössbauer line. The isomer shift, δ, the quadrupole shift, ε and the magnetic hyperfine field, H_{hf}, parameters have been obtained.

3. Results and discussion

X-ray diffraction investigations showed that the $YFe_{11}TiH_x$ ($x = 0$, 1) samples were a single phase with the $ThMn_{12}$-type structure. The crystallographic and magnetic investigations for polycrystalline samples have already been reported in reference [11]. Structural and magnetic properties of $YFe_{11}TiH_x$ ($x = 0$, 1) single crystals are summarized in table 1.

Table 1. Crystallographic and magnetic data of single crystals of $YFe_{11}Ti$ and its hydride.

Compound	a (Å)	c (Å)	V (Å^3)	$\Delta V/V$(%)	T_c (K)	M_S (μ_B f.u.$^{-1}$) ($T = 4.2$ K)
$YFe_{11}Ti$	8.509	4.783	346.6	–	538	19.3
$YFe_{11}TiH$	8.547	4.786	349.6	0.95	597	20.3

It can be seen from our experimental results that the introduction of hydrogen increases the value of T_c. This increase might be connected with a volume cell expansion. According to Li *et al* [13] there is a relation between the volume cell expansion and the increase of the Curie temperature for carbides and nitrides. The ratio

$$\rho = \frac{\Delta T_c/T_c}{\Delta V/V}$$

is 12.4 for carbides and nitrides of $YFe_{11}Ti$. For the hydride, ρ is found to be 12.7. This might be an indication that the increase in the Curie temperature we observed in the hydrides is a volume effect too.

Figure 1 shows the field dependence of the magnetization measured at 4.2 K for the $YFe_{11}Ti$ and $YFe_{11}TiH$ single crystals along the easy direction (EMD) [001] and along a hard magnetization direction (HMD) [100], respectively. The saturation magnetization and the easy c-axis anisotropy are larger upon hydrogenation. The weak anisotropy within the basal plane in the $YFe_{11}Ti$ remains negligible in the $YFe_{11}TiH$ single crystal too. Figure 2 shows the field dependence of the magnetization at several temperatures measured along the HMD for the $YFe_{11}TiH$ hydride. From the magnetization measurements along the EMD, i.e. the [001] axis, the temperature dependence of the spontaneous magnetization, M_S, has been obtained. Figure 3 shows the spontaneous magnetization of the $YFe_{11}Ti$ and $YFe_{11}TiH$ single crystals as a function of temperature. Hydrogenation leads to the increase of the M_S value. The M_S value in the $YFe_{11}TiH$ at 4.2 K is equal to 20.3 ± 0.1 μ_B f.u.$^{-1}$

In order to determine the anisotropy constants, we used the Sucksmith–Thompson relation for an easy-axis system [14]. Considering the usual phenomenological expression for the

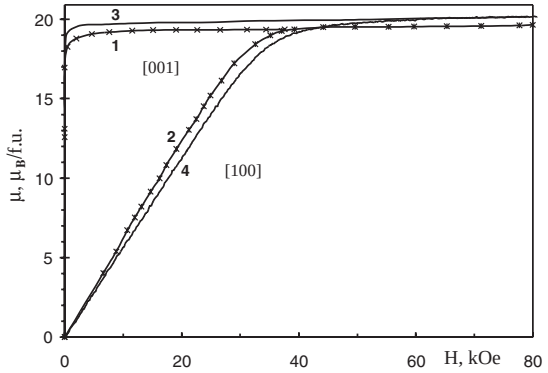

Figure 1. Field dependence of magnetization along the [001] and [100] symmetry axes at $T = 4.2$ K for $YFe_{11}Ti$ (1, 2) and its hydride (3, 4), respectively.

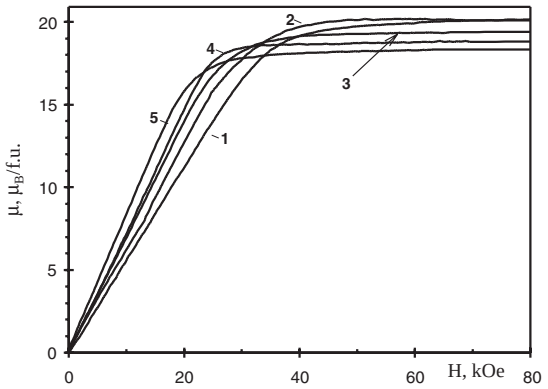

Figure 2. Magnetization isotherms for the $YFe_{11}TiH$ single crystal along the hard magnetization direction [100] at $T = 4.2$ K (1), 60 K (2), 100 K (3), 150 K (4) and 250 K (5).

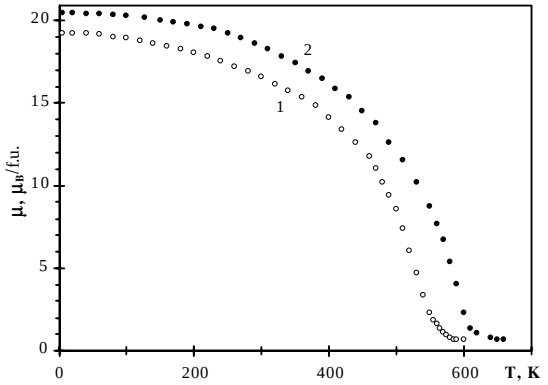

Figure 3. Temperature dependence of the spontaneous magnetization for $YFe_{11}Ti$ (1) and its hydride (2).

magnetocrystalline anisotropy of the tetragonal system and neglecting the anisotropy within the basal plane, the total energy is as follows:

$$E = K_1 \sin^2(\theta) + K_2 \sin^4(\theta) - H \cdot M_S \qquad (1)$$

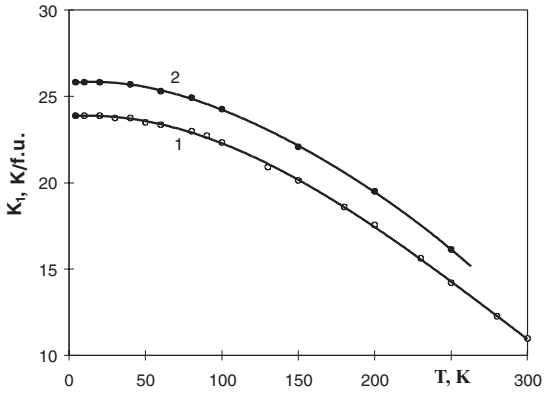

Figure 4. Temperature variation of the second-order $K_1(T)$ magnetocrystalline anisotropy constants of the $YFe_{11}Ti$ (1) and its hydride (2) (the lines are a visual guide).

where θ is the angle between the c-axis and the M_S vector. The third term represents the Zeeman energy where H is an applied field. If $H < H_A$ (where H_A an anisotropy field), the minimization of the total energy gives the field dependence of the magnetization, M in the direction of the applied field, which can be written as

$$H/M = 2K_1/M_S^2 + 4K_2 \cdot M^2/M_S^4. \tag{2}$$

By plotting H/M versusM_S^2 at the different temperatures we have obtained the values K_1 and K_2. Extrapolation of H/M for $M = 0$ gives K_1 while the slope of plots determines K_2. The temperature dependence of the second-order magnetocrystalline anisotropy constants, K_1 of the $YFe_{11}Ti$ single crystal and its hydride below 300 K are shown in figure 4. According to our experimental results the value of K_1 at 4.2 K for the $YFe_{11}TiH$ single crystal reaches 25.8 K f.u.$^{-1}$ and $K_2 = 0.24$ K f.u.$^{-1}$, respectively. The uniaxial anisotropy constant K_1 increases, while K_2 decreases slightly upon hydrogenation.

The Mössbauer spectra of $YFe_{11}Ti$ and $YFe_{11}TiH$ registered at 20 K and 295 K are shown in figure 5. Usually, the Mössbauer spectra in $ThMn_{12}$ structure were fitted with three sextets assigned to the three independent crystallographic sites occupied by Fe atoms: 8f, 8j and 8i. The relative areas of the three subspectra were constrained to be in the ratio 4:4:3 for the 8f, 8j and 8i sites, respectively. However, in [4] it was shown that such an approach cannot describe satisfactorily the complexity of the spectrum. The fact of an occupancy of the 8i sites by titanium atom in $YFe_{11}Ti$ should be taken into account [15]. The 8f, 8i and 8j sites each have Ti atoms as near neighbours randomly distributed on the 8i site. In such a case, each of three sextets must be additionally divided into three subsextets, $8f_i$, $8j_i$ and $8i_i$, where $i = 0$, 1, 2 which corresponds to an iron atom with zero, one and two titanium nearest neighbours with relative areas given by a binomial distribution of 25% titanium occupancy on the 8i site. Hence, the 8i site is represented by three sextets $8i_0$, $8i_1$ and $8i_2$ with relative areas of 7, 12 and 8%, and the 8j and 8f sites are each represented by three sextets with relative areas of 12, 16 and 8%. Thus a total of nine sextets have been used to analyse the Mössbauer spectra.

In the hydride samples this approach is the same because hydrogenation retains the crystal structure of the parent compound changing the cell volume only by about 1%. In order to assign the Mössbauer subspectra to the corresponding Fe sites we must consider the nearest-neighbour environments. For both $YFe_{11}Ti$ and $YFe_{11}TiH$, the 8i site has the largest number of iron near neighbours (11.75 on average), whereas each 8j and 8f site has only nine adjacent Fe atoms. Thus the largest hyperfine field should be for 8i site and the hyperfine fields are

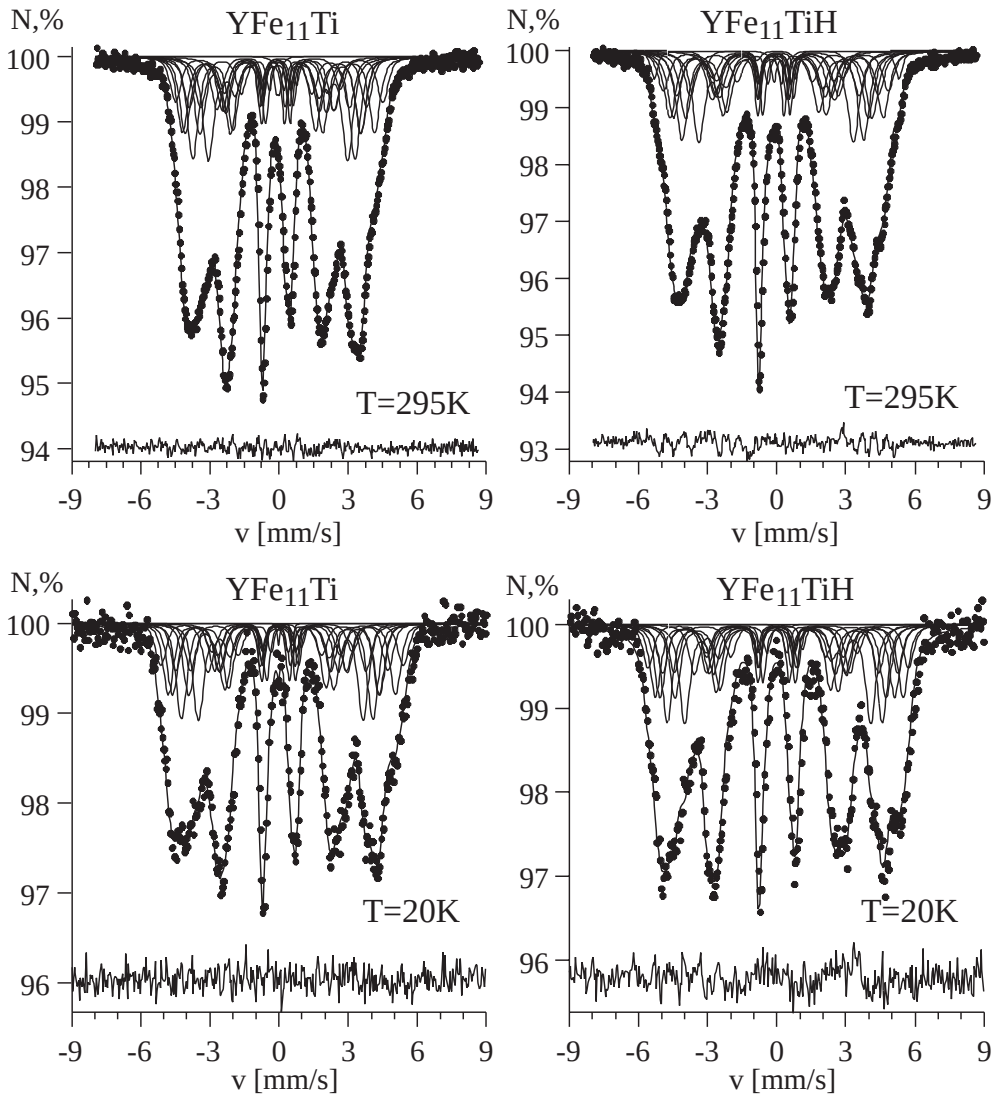

Figure 5. ^{57}Fe Mössbauer spectra of $YFe_{11}Ti$ and $YFe_{11}TiH$ at 20 and 295 K.

expected to follow the sequence $H_{hf}(8i) > H_{hf}(8j) > H_{hf}(8f)$ for both compounds. This assignment is consistent with previous Mössbauer studies of $ThMn_{12}$-type compounds [16]. The hyperfine parameters, $\langle H_n \rangle$ and $\langle \delta \rangle$, determined from the spectra taken at 20 K and 295 K are shown in figure 6 and summarized in table 2.

The hyperfine fields for all iron sites at room temperature and 20 K in the $YFe_{11}TiH$ hydride are about 30 kOe larger than in $YFe_{11}Ti$ alloy. These increases are in line with the increase in the unit cell volume, the magnetization and the Curie temperature upon hydrogenation. The hyperfine fields H_n as a function of the number of Ti neighbours for the considered cases with zero, one and two titanium near neighbours obey a simple linear relationship $H_n(m) = H_{n0} + m\Delta H$ ($m = 1, 2, 3$). In other words, the contributions from the nearest neighbours to the hyperfine field experienced by Fe nuclei are additive [17]. From the hyperfine fields,

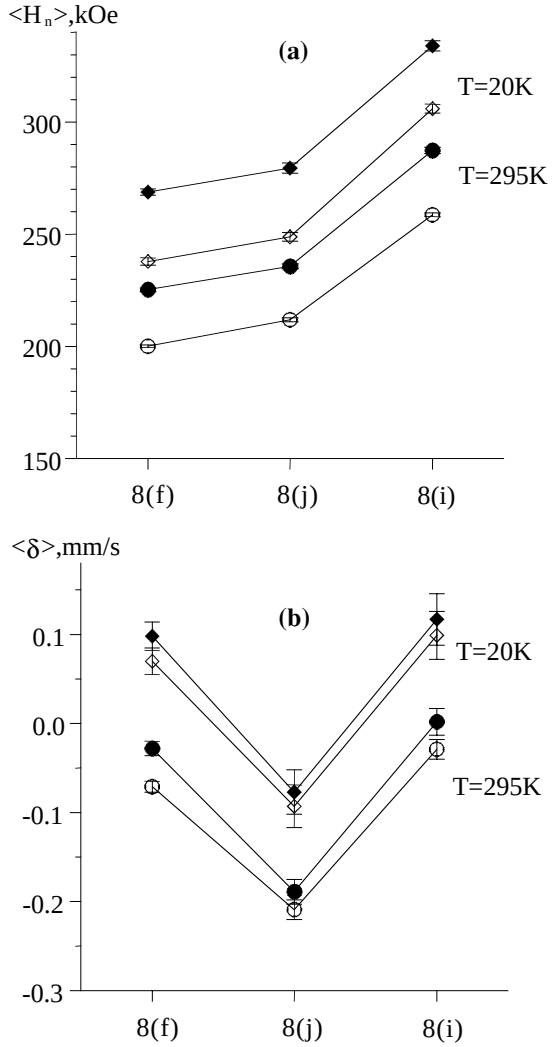

Figure 6. (a) Average hyperfine fields and (b) the isomer shifts of the three inequivalent Fe sites for $YFe_{11}Ti$ (open symbols) and its hydride (full symbols) measured at 20 and 295 K.

the values of the magnetic moments for the three inequivalent Fe sites can be obtained. If a conversion factor of 156 kOe μ_B^{-1} [9] is used, the magnetic moments of Fe at 8i, 8j and 8f sites in $YFe_{11}TiH$ hydride at 20 K can be estimated as 2.14, 1.80 and 1.72 μ_B, respectively. The weighted average value of 1.86 μ_B is in good agreement with an average magnetic moment of 1.85 μ_B calculated from our magnetization measurements.

As is seen in figure 6 the hydrogen also increases the average isomer shift in the 8i, 8j and 8f sites. Analysing these changes it appears that hydrogen atoms have an anomalous influence on an electronic state of the Fe atom in 8j site. For the 8j position the total increase in the isomer shift is less than it is for the other positions. The observed isomer shifts in the 8f and 8i sites can be accounted for by the increase of the Wigner–Seitz unit cell volumes of Fe atoms upon hydrogenation. It is known that the volume effect on the iron shift Δ IS/Δ ln$V$ for the close-packed structure is about 1.37 mm s^{-1} [18]. Unfortunately, in the case of 8j position

Table 2. Mössbauer hyperfine parameters for $YFe_{11}Ti$ and $YFe_{11}TiH$ at $T = 20$ K and 295 K. All quantities are given in mm s^{-1} except the hyperfine fields, which are given in kOe. (δ_0, ε_0 and H_0 are maximum values of the isomer shift, the quadrupole shift and the magnetic hyperfine field in the case when there is no Ti as a nearest neighbour. $\Delta\delta$, $\Delta\varepsilon$ and ΔH are the change in values of isomer shift, quadrupole shift and magnetic hyperfine field in the case when one Ti atom is present as a nearest neighbour. $\langle\delta\rangle$, $\langle\varepsilon\rangle$ and $\langle H\rangle$ are average values for the given crystallographic positions.)

		20 K		295 K	
Site	Hyperfine parameters	$YFe_{11}Ti$	$YFe_{11}TiH$	$YFe_{11}Ti$	$YFe_{11}TiH$
	δ_0	0.038 ± 0.010	0.063 ± 0.011	-0.108 ± 0.004	-0.084 ± 0.005
	$\Delta\delta$	0.035 ± 0.010	0.039 ± 0.011	-0.042 ± 0.004	0.063 ± 0.005
	$\langle\delta\rangle$	0.070 ± 0.015	0.098 ± 0.016	-0.071 ± 0.006	-0.028 ± 0.008
	ε_0	0.191 ± 0.013	0.126 ± 0.011	0.166 ± 0.005	0.103 ± 0.007
8f	$\Delta\varepsilon$	0.026 ± 0.011	0.091 ± 0.011	0.021 ± 0.005	0.122 ± 0.007
	$\langle\varepsilon\rangle$	0.214 ± 0.018	0.208 ± 0.016	0.184 ± 0.008	0.211 ± 0.011
	H_0	257.7 ± 1.2	284.8 ± 0.9	217.2 ± 0.4	246.3 ± 0.5
	ΔH	-22.3 ± 1.0	-18.0 ± 0.9	-19.3 ± 0.4	-23.6 ± 0.5
	$\langle H\rangle$	237.9 ± 1.6	268.8 ± 1.4	200.1 ± 0.6	225.3 ± 0.8
	δ_0	-0.071 ± 0.018	0.053 ± 0.018	-0.195 ± 0.008	-0.141 ± 0.009
	$\Delta\delta$	-0.024 ± 0.014	-0146 ± 0.015	-0.016 ± 0.005	-0.053 ± 0.009
	$\langle\delta\rangle$	-0.093 ± 0.024	-0.077 ± 0.025	-0.209 ± 0.011	-0.189 ± 0.014
	ε_0	-0.067 ± 0.020	-0.002 ± 0.019	-0.059 ± 0.008	-0.020 ± 0.009
8j	$\Delta\varepsilon$	-0.124 ± 0.018	-0.217 ± 0.014	-0.106 ± 0.008	-0.167 ± 0.007
	$\langle\varepsilon\rangle$	-0.177 ± 0.029	-0.195 ± 0.027	-0.153 ± 0.012	-0.169 ± 0.012
	H_0	278.6 ± 1.4	316.8 ± 1.7	237.1 ± 0.7	268.2 ± 0.9
	ΔH	-33.5 ± 1.2	-41.9 ± 1.3	-28.4 ± 0.5	-36.5 ± 0.5
	$\langle H\rangle$	248.8 ± 1.9	279.5 ± 2.3	211.9 ± 0.9	235.7 ± 1.1
	δ_0	0.136 ± 0.018	0.170 ± 0.019	0.032 ± 0.007	0.013 ± 0.009
	$\Delta\delta$	-0.036 ± 0.018	-0.052 ± 0.020	-0.059 ± 0.007	-0.011 ± 0.009
	$\langle\delta\rangle$	0.099 ± 0.027	0.117 ± 0.029	-0.029 ± 0.011	0.002 ± 0.015
	ε_0	-0.011 ± 0.017	-0.076 ± 0.018	-0.024 ± 0.007	-0.044 ± 0.009
8i	$\Delta\varepsilon$	0.038 ± 0.017	0.094 ± 0.020	0.033 ± 0.007	-0.047 ± 0.009
	$\langle\varepsilon\rangle$	0.028 ± 0.026	0.021 ± 0.029	0.010 ± 0.011	0.004 ± 0.014
	H_0	327.2 ± 1.4	351.5 ± 1.5	279.5 ± 0.5	303.6 ± 0.9
	ΔH	-20.6 ± 1.2	-17.0 ± 1.5	-20.2 ± 0.5	-15.8 ± 0.9
	$\langle H\rangle$	306.0 ± 2.0	334.0 ± 2.3	258.7 ± 0.8	287.4 ± 1.4

the Wigner–Seitz unit cell volume diminishes from 12.31 to 11.01 Å upon hydrogenation and the volume effect should rather decrease the isomer shift value. Therefore, the measured isomer shift value indicates that another phenomenon, opposite to the volume effect, affects the isomer shift of Fe nuclei on the 8j sites. This contribution to the isomer shift of Fe(8j) nuclei can be attributed to the transfer of the s-electrons from Fe to the adjacent hydrogen atoms. Neutron diffraction studies [19] show that hydrogen atoms occupy the 2b site in the $ThMn_{12}$ structure as is shown in figure 7. Four iron atoms in 8j sites in ab plane surround a hydrogen atom. Table 3 shows the distances between appropriate sites in $YFe_{11}TiH$ and $YFe_{11}Ti$. The largest interatomic distances of H atoms are between Fe(8i) atoms (3.78 Å) and Fe(8f) atoms (3.25 Å) whereas the smallest ones are between Fe(8j) atoms (1.86 Å).

The short bonds between 8j (Fe) and the interstitial hydrogen facilitate strong hybridization. The observed increase of the isomer shift on the Fe(8j) nuclei over its expected

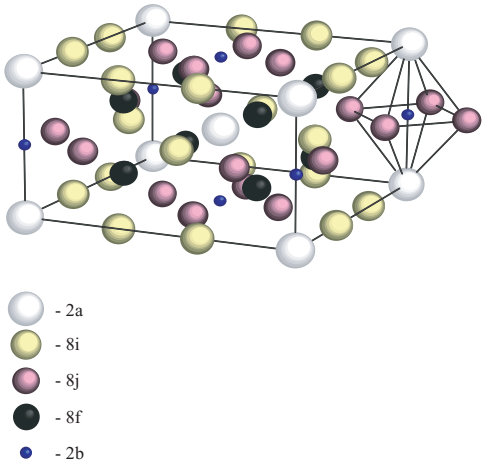

Figure 7. $ThMn_{12}$ structure showing the 2b interstitial sites which can be seen as a pseudo-octahedron with two rare earth elements and four iron atoms at the corners.

Table 3. The interatomic distances (in Å) and the numbers of adjacent atoms for each site (values in the brackets are for $YFe_{11}Ti$).

Site	$d_{Fe–Fe}$	$d_{Fe–Y}$	$d_{Fe–H}$	$n_{Fe–Fe} + n_{Fe–Y} + n_{Fe–H}$
8i	2.68(2.67)	2.93(2.92)	3.78	13 + 1 + 1
8j	2.64(2.62)	3.03(3.03)	1.86	10 + 2 + 1
8f	2.39(2.39)	3.25(3.24)	3.25	10 + 2 + 2

diminution caused by the volume effect reflects the decrease of the s-electron density on this position with hydrogen insertion.

Finally, it is worth noting that the change of the isomer shift by -0.12 ± 0.02 mm s^{-1} between 20 K and 295 K for both $YFe_{11}Ti$ and its hydride is in agreement with second-order Doppler effect for a Debye temperature of $\theta_D = 330$ K [20].

4. Conclusion

We have made a systematic study of the influence of hydrogen on the structure and magnetic properties of $YFe_{11}Ti$. It is found that most of the magnetic properties (Curie temperature, Fe moment, the easy *c*-axis anisotropy) are enhanced upon hydrogenation. The obtained results for $YFe_{11}Ti$ and $YFe_{11}TiH$ single crystals should be useful in an analysis of the magnetocrystalline anisotropy and the Mössbauer spectra of similar compounds containing magnetic rare earth atoms.

Acknowledgments

We are indebted to K P Skokov, V V Zubenko, I V Telegina, N Yu Pankratov for the preparation of the single crystals and useful discussions. We also thank F G Vagizov for his remarks. The work has been supported by RFBR Grant No 99-02-17821.

References

[1] Qi-nian Qi, Li Y P and Coey J M D 1992 *J. Phys.: Condens. Matter* **4** 8209
[2] Soubeyroux J L, Fruchart D, Isnard O, Miraglia S and Tomey E 1995 *J. Alloys Comp.* **219** 16
[3] Obbade S, Miraglia S, Fruchart D, Pre M, L'Heritier P and Barlet A 1998 *CR Acad. Sci. Paris Ser. II* **307** 889
[4] Obbade S, Fruchart D, Bououdina M, Miraglia S, Soubeyroux J L and Isnard O 1997 *J. Alloys Comp.* **253/254** 298
[5] Yang J, Domg S, Mao W, Xuan P and Yang Y 1995 *Physica* B **205** 341
[6] Pröbst F and Wagner F E 1987 *J. Phys. F: Met. Phys.* **17** 2459
[7] Schneider G, Baier M, Wordel, Wagner F E, Antonov V E, Poniatovsky E G, A Lopilovskii Yu and Makarov E 1991 *J. Less-Common Met.* **172–174** 333
[8] Zhang B, Bauer H J, Baier M, Wagner F E, Antonov V E and Antonova T E 1991 *J. Less-Common Met.* **172–174** 343
[9] Hu B P, Li H S, Gavigan J P and Coey J M D 1989 *J. Phys.: Condens. Matter* **1** 755
[10] Abadia C, Algarabel P A, Garcia-Landa B, Ibarra M R, Del Moral A, Kudravatykh N V and Markin P E 1998 *J. Phys.: Condens. Matter* **10** 349
[11] Nikitin S A, Tereshina I S, Verbetsky V N and Salamova A A 1998 *Fiz. Tv. Tela* **40** 285 (in Russian)
[12] Tereshina I S, Nikitin S A, Ivanova T I and Skokov K P 1998 *J. Alloys Comp.* **275–277** 625
[13] Li Z W, Zhou X Z and Morrish A H 1993 *J. Phys.: Condens. Matter* **5** 3027
[14] Sucksmith W and Thompson J E 1954 *Proc. Roy. Soc.* (London) **225** 362
[15] Li Z W, Zhou X Z, Morrish A H and Yang Y C 1990 *J. Phys.: Condens. Matter* **2** 4253
[16] Yang J, Ding Y, Zhang B, Ye C, Jin and Zhou H 1988 *J. Appl. Phys.* **64** 5968
[17] Rusakov V S, Iljushin A S, Morozov V N and Nikanorova I A 1994 *Izv. Akad. Nauk* Ser. Fizicheskaya **58** 24 (in Russian)
[18] Williamson D L, Bukshpan S and Ingalls R 1972 *Phys. Rev.* B **6** 4194
[19] Weihua M, Jinbo Y, Bo C, Benpei C, Yingchang Y, Honglin D, Baisheng Z, Chuntang Y and Jilian Y 1998 *J. Phys.: Condens. Matter* **10** 2611
[20] Bodrjakov V Yu and Nikitin S A 1995 *Fizika metallov i metallovedenie* **80** 62 (in Russian)